# Socioeconomic impact of COVID-19 restrictions in Bali: A nighttime light analysis

Dimas Hutomo Putro[a*], Setia Pramana[b], Daffa Hendrawan[c]
[a]*BPS-Statistics of Jakarta, Jakarta, Indonesia*
[b]*Politeknik Statistika STIS, Jakarta, Indonesia*
[c]*BPS-Statistics of Nagekeo Regency Office, East Nusa Tenggara, Indonesia*

Submitted: 07 August 2022 – Revised: 10 March 2025 – Accepted: 20 April 2025

## Abstract

This study investigates the socio-economic impacts of COVID-19 pandemic restrictions in Bali using nighttime light remote sensing as a proxy for socio-economic activity. The monthly NTL data from the Suomi-NPP VIIRS instrument, spanning from 2014 to 2021, are analyzed. This study focuses on changes in NTL trends before and after the restrictions, specifically the Large-Scale Social Restriction and Welfare Activity Restriction programs. To ensure that the NTL used in this study accurately measures human activity, we integrate the data with built-up area maps from the Global Human Settlement Layer. An ARIMA intervention model is employed to assess the impact of the restrictions on NTL, revealing a significant decrease in certain regions. Furthermore, we find a moderate correlation between NTL and Bali's quarterly GDP data. This study also highlights the potential of NTL remote sensing as a near-real-time proxy for socioeconomic change, allowing for the early evaluation of policy effectiveness.

**Keywords:** nighttime light, COVID-19, proxy indicator, ARIMA intervention
**JEL Classification:** C22; I18; R11

**Recommended Citation**
Pramana, Setia; Putro Dimas Hutomo (2025). *Socioeconomic impact of COVID-19 restrictions in Bali: A nighttime light analysis*. Jurnal Ekonomi Indonesia. 14 (1), 2025: 93-110. DOI: https://doi.org/10.52813/jei.v14i1.220

Available at: https://jurnal.isei.or.id/index.php/isei



*Corresponding Author : dimas.hutomo@bps.go.id

# 1. Introduction

The COVID-19 pandemic, beginning in late 2019 (WHO, 2020), caused widespread social and economic disruptions globally. The virus, SARS-CoV-2, which causes the pandemic, easily transfers through the air and quickly spreads, infecting humans as its hosts. In Indonesia, the first case was reported in March 2020 (Almutaqi, 2020), leading to various levels of restrictions: *pembatasan sosial berskala besar* – PSBB (large-scale social restriction program - LSSRP) and *pemberlakuan pembatasan kegiatan masyarakat* – PPKM (welfare activity restriction program - WARP), both implemented in Bali. These restrictions applied after local and national regulations, respectively: *Governor's Instruction No. 8851 of 2020* and *Minister of Home Affairs Instruction No. 01 of 2021,* by limiting the community's outdoor activity.

The economy of Bali, which heavily relies on tourism, was affected by the restrictions mentioned. The National Bureau of Statistics (BPS) in 2022 stated that the growth of Bali's GDP tends to slow down. (BPS, 2022). Prior to the pandemic, the GDP tended to increase. It illustrates the drastic decline in socio-economic activity following the implementation of travel restrictions. These restrictions, while necessary, presented a dilemma: balancing public health with economic stability (Haavelmo & Hansen, 1991). Therefore, government efforts are needed to evaluate the restrictions' impact on the community's socio-economic well-being.

Generally, efforts to measure the socioeconomic conditions of the community rely on data sourced from official statistics. However, official statistics have the possibility of a time lag, so that data for policymaking may become unavailable. The delay may cause essential information for policymaking to become outdated. In addition, the process of traditional data collection, such as face-to-face interviews, was not recommended due to the high risk of virus spread (WHO, 2020) Therefore, alternative data sources are needed with the following criteria: availability in a more timely period, similarity or likely related official statistics, and the ability to complement information from official statistics. In other words, these data sources can be used as a proxy indicator for data sourced from official statistics.

To overcome the limitations of traditional data sources, several alternative data sources can be employed to assess the socio-economic activities of the community, One promising option is nighttime light (NTL) satellite imagery. NTL remote sensing offers a different perspective by capturing light emissions, which are strongly correlated with human activity and economic conditions (Levin, et al., 2020); (Devkota, Miyazaki, Witayangkurn, & Kim, 2019); (Li, Li, Xu, & Wu, 2017). Besides that, the use of NTL data, acquired by satellites like Suomi-NPP with its visible infrared imaging radiometer suites (VIIRS) instrument (Elvidge, Baugh, Zhizhin, Hsu, & Tilottama, 2017) Provides a cost-effective and efficient way to monitor these changes over time. Furthermore, NTL demonstrates its ability to detect changes over time during Hurricane Irma and Maria (Zhao, et al., 2020). Karimah and Yudhistira (2020) Also stated that NTL can detect local economic activity 1.8% increase in NTL intensity due to small port openings. Moreover, NTL data has been used as a proxy indicator of national, regional, and urban Gross Domestic Product (Mellander, Lobo, Stolarick, & Matheson, 2015)

Based on the fact that GDP can be proxied by NTL, this study investigates how the GDP, as a measure of socio-economic activity of the province of Bali, correlates with

NTL. Furthermore, this research examines how activity restrictions during COVID-19 in Bali impacted its socio-economic activity. To explore relationships and impacts, this study uses alternative data sources of nighttime light satellite imagery as a proxy indicator to measure changes in socio-economic activities in Bali, for the period 2014 – 2021, with the hope of being able to see pre-pandemic activities and the peak pandemic period when restrictions were applied. This study aims to assess how the impact of social restrictions on the socio-economy of the community is seen from changes in NTL trends. Hence, this study uses an autoregressive integrated moving average (ARIMA) intervention to model and measure the change in NTL based on the social restrictions mentioned. The approach of using ARIMA intervention is used to accommodate the nature of NTL, which has an abrupt change in its series without masking the image.

Before modelling the NTL with ARIMA, this study first examined the correlation between GDP and NTL to validate the NTL as a reliable socio-economic proxy. After measuring the closeness, we then proceeded with ARIMA intervention model to provide an overview of whether NTL as an alternative data source can be used as a proxy and/or complementary indicator that enriches the results of traditional data collection with official statistics so that it can provide an insight for policymakers related to socio-economic disruption during crises like COVID-19.

## 2. Methodology

This study uses remotely sensed NTL data from Earth Observation Group, which processed daily nightlight images collected from Suomi National Polar-orbiting Partnership (Suomi-NPP) Satellite. The image is collected with the Visible Infrared Imaging Radiometer Suite (VIIRS) sensor. This data is available from the Google Earth Engine data catalog. This study replicates the NTL acquisition method from Open Nighttime Lights by World Bank.

Data processed in the geographic information system (GIS) program produces output data in the form of images. To perform analysis, it is necessary to change information from images into numbers. The stage of taking information from an area in an image to make it a number that can be analyzed is called the reducing process. The reducing process is carried out by aggregating the values of each pixel in the image based on the area of interest, as illustrated in Figure 1 (Gorelick, et al., 2017). This stage reduces information from all pixels in the image into basic statistical data in the form of total value, average, median, minimum, or maximum value. The NTL total value, or the Sum of Lights (SOL), was chosen to be the data in this study because it represents the total amount of activity within the area of interest (Han, Zhou, Sun, & Zhu, 2022).

**Figure 1.** Reducing process in Google Earth Engine


Source: Author documentation

VIIRS captures every light reflection on earth, whether it is a source of light or any other object, such as light reflection from vegetation and water bodies. To ensure there is no bias in the area of interest, a map containing the areas inhabited by humans is required in this study. Eurostat creates a map that presents human settlement areas, known as the Global Human Settlement Layer (GHSL). This map is compiled from images produced by Landsat satellites and processed using a machine-learning classification algorithm. This data can be used as additional information on other images that require classification support (Pesaresi, et al., 2016). GHSL consists of two types, namely built-up areas (GHSL Built Up Grid) and population plots (Population Grid). GHSL offers a map of built-up areas and the population density of development in various regions. The data presented, as shown in Figure 2, are areas and population density from 1975, 1990, 2000, and 2014 (Pesaresi M. , et al., 2016). Since this research is mainly focused on community activity, a built-up area is chosen.

**Figure 2.** Illustration of GHSL Built-up Grid compared to satellite view

Source: Author documentation derived from GHSL Built-up

After identifying built-up areas using GHSL, the next step is to apply a masking process to the NTL images to isolate human settlements. This process is illustrated in Figure 3

**Figure 3.** Illustration of masking process using NTL images and GHSL Built-Up


Source: Author documentation derived from VIIRS imagery

After applying the GHSL mask, the VIIRS image is further divided into several regencies. A shapefile layer from *Badan Pusat Statistik* is used to delineate borders between regencies, so that the analysis can be done in a lower level. This process is carried out repeatedly so that monthly NTL data for every regency in Bali from January 2014 to December 2021 is obtained (Figure 3).

The official statistical data are also used in this study. This data is used for comparison to the obtained data from VIIRS with the official statistics to study the possibility of NTL being used as a proxy indicator and/or complement the official statistics data. The quarterly GDP for the province of Bali, spanning from 2014 to 2021, is used as official statistical data as a comparison to the NTL. These data were selected because of the ability to represent NTL and dominant socio-economic activities (Mellander, Lobo, Stolarick, & Matheson, 2015).

Correlation is a close relationship between two linear variables. Generally, the close relationship between two variables can be found using Pearson and Spearman correlations (Cohen, 1988). In this study, Pearson correlation was not used because time series data tends to depend on time (Box, Jenkins, Reinsel, & Ljung, 2015). Ye, et al. (2015) Suggest using Spearman to see the closeness between two time series variables. Therefore, this study uses the Spearman correlation calculation method to avoid bias that may arise due to using the Pearson correlation calculation. This calculation uses the actual value of the available data quantity as the basis for calculation. The result of the correlation measurement is a quantity that states the relationship between the two variables whose closeness is sought. It is important to note that while measuring closeness between two time series data correlation does not imply causal or linearity in the relationship, because the time series has autocorrelation and might lead to spurious correlation (Ye, Xiao, Esteves, & Rong, 2015).

Spearman's correlation coefficient can be obtained from the equation below:

$$r_S = 1 - \frac{6\sum_{i=1}^{N} d_i^2}{N(N^2-1)} \quad (1)$$

With $d_i$ is difference of two rankings between paired data and N is the number of paired data.

In analyzing time series data, sudden changes can occur due to policies implemented at specific points in time. Policies that occur could impact and change the time series data structure, so it is necessary to model the event and the effect of the intervention (Shmueli & Lichtendahl Jr., 2016). According to Box and Tiao in Montgomery & Jennings (2015), intervention analysis is an attempt to find out the response of a variable when there is an event whose period is specifically known.
ARIMA intervention is a special case of a dynamic linear regression model, as stated by Makridakis, Wheelwright, & Hyndman (1997)

To analyze using ARIMA and the intervention model, the monthly NTL data is divided into three parts:

1) Data before intervention of the first restriction, (January 2014 to March 2020);
2) Data after the first intervention of the first restriction after *Governor's Instruction No. 8851 of 2020* as local regulation for implementing LSSR, (April 2020 to December 2020), where $T = 76$; and

3) Data after the second intervention of the first restriction after *Minister of Home Affairs Instruction Number 01 of 2021* as a regulation for implementing WARP, (January 2021 to December 2021) $T = 85$.

The data before intervention is modelled using seasonal autoregressive integrated moving average (SARIMA), which follows Box-Jenkins method and finds the best model that follows Hyndman-Khandakar algorithm (2008). The steps in this study are as follows:

1) Visual inspections,
2) Transforming the data as needed,
3) Model selection based on Hyndman-Khandakar

In general, the SARIMA$(p, d, q)(P, D, Q)$ model follows:

$$y_t = c + \frac{(1+\theta_1 B+\cdots+\theta_q B^q)(1+\Theta_1 B+\cdots+\Theta_Q B^Q)}{(1-\Phi_1 B-\cdots-\Phi_P B^p)(1-B)^d(1-B)^D}\varepsilon_t \quad (2)$$

Then, data before intervention are forecasted until the end of the first intervention, if the residual shows a significant difference from the ±2 times standard deviation range. The order of transfer functions is b, r, and s. The b denotes the first residual time lag after intervention, r denotes the residuals pattern (0 if no pattern, 1 if exponential, and 2 if the pattern shows a sine wave), and s denotes the length of intervention. The transfer function and the ARIMA model can be written as:

$$y_t = \frac{\omega(B)}{\delta(B)}\xi_t^{(T)} + \frac{\theta(B)}{\phi(B)}\varepsilon_t \quad (3)$$

A simplified form of the intervention model can be derived from the previous transfer function representation.

$$y_t = v(B)\xi_t^{(T)} + N_t \quad (4)$$

Where $y_t$ denotes the response variable at time $t$; $\xi_t^{(T)}$ denotes the intervention variable at time $t$ with value 1 at time T, which follows a step or pulse process; $v(B)$ denotes transfer function $\omega$ and $\delta$ denotes moving average and respectively at the transfer function that has order of b, r, s; and $N_t$ denotes ARIMA model before intervention.

The pulse function can be written as:

$$\xi_t^{(T)} = S_t^{(T)} = \begin{cases} 0, t \neq T \\ 1, t = T \end{cases} \quad (5)$$

While the step function can be written as:

$$\xi_t^{(T)} = P_t^{(T)} = \begin{cases} 0, t < T \\ 1, t \geq T \end{cases} \quad (6)$$

The step function is typically used if the intervention is permanent, while the pulse function is used while the intervention is temporary.

To inspect the existence of second intervention, the model formed before is forecasted one more time. If the response shows a significant difference from 2 2-

standard-deviation range, then it is modelled using a transfer function following the step above. After fitting the model, we perform Ljung-Box test statistic to check whether the ARIMA model has perfectly handled the serial correlation in the time series data. The test statistics can be written as:

$$Q_{LB} = T(T+2)\sum_{k=1}^{K}\left(\frac{1}{T-k}\right)r_k^2 \quad (7)$$

The model is selected if $Q_{LB} < \chi^2_{(K-p-q)}$, or has p-values larger than 5%, which means the model has handled the serial correlation in the time series data.

## 3. Results and Discussion

### 3.1. Overview of NTL data in the Province of Bali

In general, the province of Bali experienced a consistent increase in SOL from early 2014 to early 2020. However, after the implementation of local restrictions in the Province of Bali in April, there was a decrease in night light with a permanent impact until the end of 2020.

The value of NTL in Bali Province began to increase in 2021 but fell again at the end of the year. In Figure 4 it can also be seen that there was an extreme decline at some points in certain years. This decline occurred in 2017, 2018, and some point in 2021.

**Figure 4.** Monthly NTL values of Bali from January 2014 to December 2021

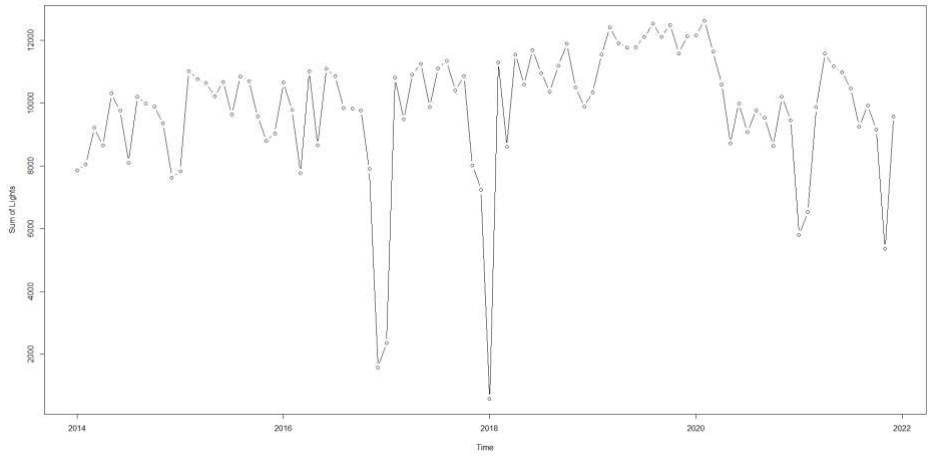


Source: Author documentation derived from VIIRS DNB imagery

To further explore the patterns observed, the analysis was extended to the city and regency levels in Bali.

**Figure 5.** Monthly NTL values from January 2014 to December 2021 for every city and regency in Bali

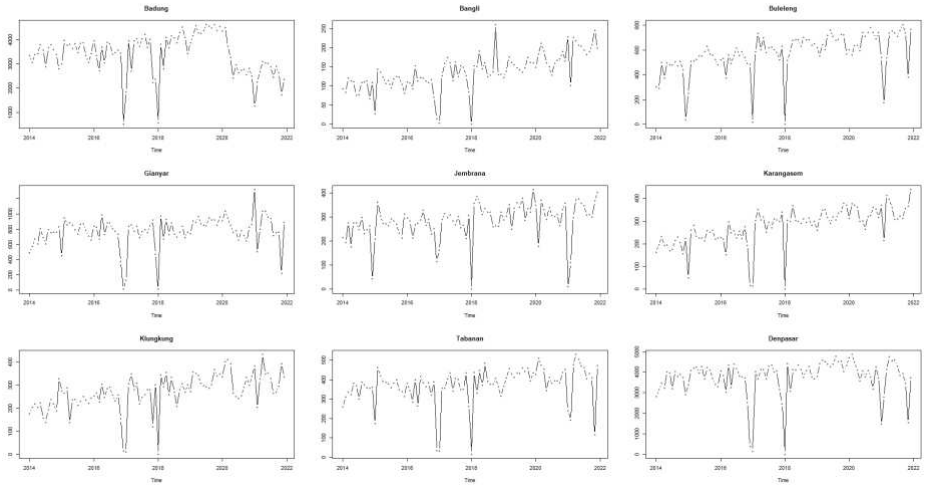


Source: Author documentation derived from VIIRS DNB imagery

Furthermore, SOL observations were carried out for each district and city in the province of Bali. Based on Figure 5, it can be seen that Badung regency and Denpasar city have the highest SOL values compared to other regions in Bali. The order of SOL values is followed by the regencies, namely Gianyar, Buleleng, and Tabanan. Badung and Denpasar had the highest declines at these time points. From the beginning of 2020 to the end of 2021, there was a permanent decline in the value of SOL in Badung and Denpasar regencies. The highest decline during this period was experienced by Badung regency.

From Figure 4 and 5, it can also be seen that there was a sharp decline at certain time points in 2017, 2018, and 2021. To make sure what happens at the time points mentioned, we examine the NTL images visually. From the results shown in Figure 6, we can say that in the previous graph that the decreasing value is caused by the bad quality of the images. This happened because the NTL that is used in this study has already masked the presence of clouds, which means the area with cloud cover is removed (Kopp, et al., 2014).

**Figure 6.** Samples of low-quality images being masked caused by cloud cover in the dataset

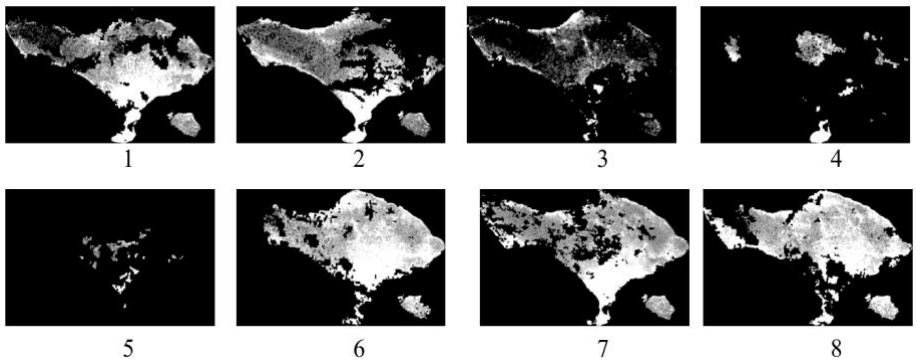


Source: Author documentation derived from VIIRS DNB imagery

Furthermore, observations were made on the data that was formed on an annual basis. In general, from year to year the value in almost every region does not change in the light emission, this is indicated by the yellow area in Figure 7. However, some areas experience an increase in light emission. Based on Figure 7, it is known that there was a quite drastic decline from 2015 to 2016 which was evenly distributed in each region. After that, from 2016 to 2017, many areas experienced an increase in the sum of lights value.

Based on the annual image formed, it can be said that NTL images at the end of 2016, 2017, and early 2021 the quality of the resulting image for all regions on the island of Bali was not good due to most of the regions being masked. Still regarding the annual image, there is also a pattern of decline in the value of the resulting image from 2019 to 2020 and 2020 to 2021, especially in Denpasar city and in the buffer areas of the capital city of Bali, namely Badung, Gianyar, and Tabanan regencies. It also indicates that most of the built-up area is located in Denpasar and Badung.

**Figure 7.** Annual NTL changes in Bali

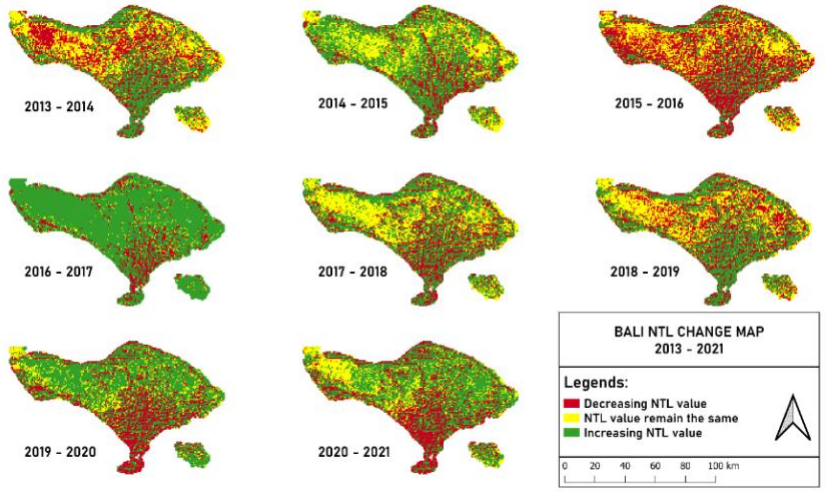


Source: Authors documentation, derived from VIIRS DNB imagery

To further analyze the correlation between NTL and GDP, we use the GDP data available from Statistics Indonesia (BPS). Given that the available data is quarterly, we add up the sum of lights each quarter so that there is a match between GDP and NTL data for each month. The graph generated from the satellite imagery was then compared with GDP data from the province of Bali, as seen in Figure 8. From visual inspection, the GDP and NTL data have a similar upward trend in the early years of 2014 to 2019 followed by a decline in 2020. From this data, we also attempted to find their correlation using the Spearman's correlation coefficient model, the results are 0.695, which showed that the correlation between NTL and GDP exists, even though the value is low.

**Figure 8.** Quarterly GDP vs NTL

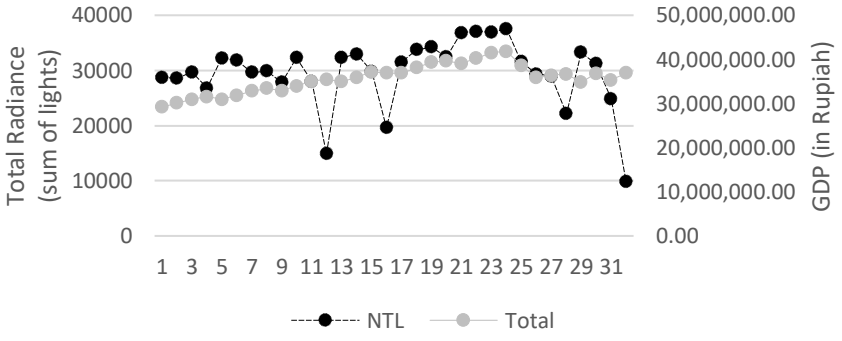


Source: Processed from Statistics Indonesia (BPS, 2024) and VIIRS DNB imagery.

Based on this correlation, we assessed that the obtained NTL can represent GDP and is consistent with the statement from Mellander, Lobo, Stolarick, & Matheson

(2015) and Elvidge et al. (2017) that NTL is related to GDP. Based on this result, we attempted to assess the socio-economic impact in Bali. The effort to correlate NTL with GDP was only applied to the province of Bali as a whole because data with a shorter time range for regencies/cities is not available. Therefore, we considered the provincial-level GDP to represent the GDP in lower-level administrative areas.

## 3.2. Measuring the Impact of COVID-19 Restrictions on Socio-Economic Activity in Bali

The ARIMA intervention model is employed to analyse the impact of a restriction policy on the province of Bali and its cities and regions. The pre-intervention data from January 2014 to March 2020, which shows outliers, were pre-processed using tsoutliers in R (R Package tsoutliers: Detection of Outliers in Time Series, 2019). This package implements the Chen and Liu outlier detection algorithm. By using this package, we mainly focused on removing the additive outliers in pre-intervention data since the remotely sensed image in this study was not masked. Iterative refinement was performed on the entire pre-intervention dataset until no further outliers were detected, corresponding to the outlier illustrated in Figure 6. Subsequently, an ARIMA model was fitted to the pre-intervention data. A forecast was then generated, and the difference between the forecast and the observed data was calculated to quantify the intervention effect. For areas anticipated to be significantly affected by the restriction policy, the magnitude of this impact was determined. The estimation results are presented in Table 1 while the full model presented in Appendix.

**Table 1.** ARIMA and intervention estimation for every city and region in Bali

| City/Region | Para-meters | Estimates | Std. Error | p-values | $Q_{LB}$ |
|---|---|---|---|---|---|
| Bali | $\theta_1$ | -0.788 | 0.080 | <0.01 | |
| | $\Phi_1$ | 0.959 | 0.122 | <0.01 | |
| $SARIMA\ (0,1,1)(1,0,1)_{12}$ $S^{(76)}\ (b=0,s=0,r=0)$ | $\Theta_1$ | -0.804 | 0.306 | <0.01 | |
| | $\omega_0^{(76)}$ | -3640.634 | 815.399 | <0.01 | |
| Badung | $\theta_1$ | -0.838 | 0.055 | <0.01 | |
| | $\Theta_1$ | 0.998 | 0.031 | <0.01 | |
| $SARIMA\ (0,1,1)(1,0,1)_{12}$ $S^{(76)}\ (b=0,s=0,r=0)$ | $\Phi_1$ | -0.964 | 0.232 | <0.01 | |
| | $\omega_0^{(76)}$ | -626.652 | 73.004 | <0.01 | |
| Bangli | $\theta_1$ | -0.726 | 0.093 | <0.01 | |
| | $\Phi_1$ | 0.916 | 0.067 | <0.01 | |
| $SARIMA\ (0,1,1)(1,0,1)_{12}$ $P^{(85)}\ (b=0,s=1,r=0)$ | $\Theta_1$ | -0.615 | 0.151 | <0.01 | |
| | $\omega_0^{(85)}$ | 86.754 | 25.207 | <0.01 | |
| | $\omega_1^{(85)}$ | -127.144 | 24.847 | <0.01 | |
| Buleleng | $\theta_1$ | -0.738 | 1125.000 | <0.01 | |
| | $\theta_2$ | -0.033 | 1486.000 | 0.82 | |
| $SARIMA\ (0,1,3)(1,0,0)_{12}$ $P^{(85)}\ (b=1,s=0,r=0)$ | $\theta_3$ | -0.112 | 1196.000 | 0.35 | |
| | $\Phi_1$ | 0.390 | 113.000 | <0.01 | |

| City/Region | Para-meters | Estimates | Std. Error | p-values | $Q_{LB}$ |
|---|---|---|---|---|---|
| | $\omega_0^{(85)}$ | -251.512 | 701.319 | <0.01 | |
| Gianyar | $\theta_1$ | -0.836 | 662.000 | <0.01 | |
| $SARIMA\ (0,1,1)(1,0,1)_{12}$ | $\Phi_1$ | 0.875 | 2777.000 | <0.01 | |
| $S^{(76)}\ (b=0,s=0,r=0)$ | $\Theta_1$ | -0.723 | 3994.000 | 0.07 | |
| $P^{(85)}\ (b=0,s=0,r=0)$ | $\omega_0^{(76)}$ | -164.683 | 636.528 | <0.01 | |
| | $\omega_0^{(85)}$ | 613.451 | 1043.643 | <0.01 | |
| Jembrana | $\theta_1$ | 0.247 | 0.111 | 0.03 | |
| | $\theta_2$ | 0.241 | 0.116 | 0.04 | |
| $SARIMA\ (0,0,2)(2,1,0)_{12}$ | $\Phi_1$ | -0.570 | 0.123 | <0.01 | |
| $P^{(85)}\ (b=0,s=1,r=0)$ | $\Phi_2$ | -0.180 | 0.136 | 0.19 | |
| | $\omega_0^{(85)}$ | -374.012 | 162.644 | 0.02 | |
| | $\omega_1^{(85)}$ | -457.756 | 154.380 | <0.01 | |
| Karangasem | $\theta_1$ | -0.651 | 0.120 | <0.01 | |
| | $\theta_2$ | -0.035 | 0.118 | 0.76 | |
| $SARIMA\ (0,1,3)(2,0,0)_{12}$ | $\theta_2$ | -0.180 | 0.104 | 0.08 | |
| $P^{(76)}\ (b=0,s=0,r=1)$ | $\Phi_1$ | 0.155 | 0.095 | 0.10 | |
| $P^{(85)}\ (b=1,s=0,r=0)$ | $\Phi_2$ | 0.392 | 0.101 | <0.01 | |
| | $\delta_1^{(76)}$ | 0.272 | 0.044 | <0.01 | |
| | $\omega_0^{(76)}$ | -42.362 | 108.818 | 0.70 | |
| | $\omega_0^{(85)}$ | -458.105 | 107.078 | <0.01 | |
| Klungkung | $\theta_1$ | -0.828 | 0.074 | <0.01 | |
| | $\Phi_1$ | 0.394 | 0.333 | 0.24 | |
| $SARIMA\ (0,1,1)(1,0,1)_{12}$ | $\Theta_1$ | -0.052 | 0.376 | 0.89 | |
| $S^{(76)}\ (b=1,s=0,r=0)$ | $\omega_0^{(76)}$ | -78.152 | 37.116 | 0.04 | |
| $P^{(85)}\ (b=1,s=0,r=0)$ | $\omega_0^{(85)}$ | -152.351 | 55.820 | <0.01 | |
| Tabanan | $\theta_1$ | -1.000 | 0.050 | <0.01 | |
| | $\Phi_1$ | -0.663 | 0.088 | <0.01 | |
| $SARIMA\ (0,1,1)(1,1,0)_{12}$ | $\delta_1^{(85)}$ | 0.506 | 0.079 | <0.01 | |
| $P^{(85)}\ (b=0,r=1,s=0)$ | $\omega_0^{(85)}$ | -31.544 | 125.999 | 0.01 | |
| Denpasar | $\theta_1$ | -0.793 | 0.087 | <0.01 | |
| | $\Phi_1$ | 0.796 | 0.151 | <0.01 | |
| $SARIMA\ (0,1,1)(1,0,1)_{12}$ | $\Theta_1$ | -0.562 | 0.205 | <0.01 | |
| $S^{(76)}\ (b=0,r=0,s=0)$ | $\omega_0^{(76)}$ | -374.092 | 116.490 | <0.01 | |
| $P^{(85)}\ (b=0,r=1,s=0)$ | $\delta_1^{(85)}$ | 0.319 | 0.068 | <0.01 | |
| | $\omega_0^{(85)}$ | -654.009 | 173.069 | <0.01 | |

Source: Processed by Author
Note: The p-value used is 0.05. p-values lower than 0.01 is written as <0.01

Overall, the estimated result parameters formed were significant and had a normal residual distribution. From the existing parameters, several regions experienced the impact of restrictions that began to be felt at time point 76 in April 2020, namely LSSR. The regions affected by the first restriction included Badung, Denpasar, Karangasem,

Klungkung, and Gianyar. These regions experienced an impact in the form of a permanent change in the resulting nighttime light emissions. The remaining regions only felt the impact of restrictions upon the implementation of WARP, or at time point 85 in January 2021. The regions that newly felt the impact at this time point included Tabanan, Jembrana, Buleleng, and Bangli. Furthermore, from the estimation results obtained, the calculation of the intervention impact magnitude was performed for both time points. The calculation of the impact magnitude was done by finding the forecasted values and subtracting them from the actual values. This impact magnitude is presented in percentage values for ease of interpreting the data magnitude. The results of the magnitude calculation are available in Table 2, Table 3, and Table 4 below.

**Table 2.** Magnitude of NTL on Region Affected by First intervention and Continued Until Second Intervention (percent)

| | Bali | | Badung | |
|---|---|---|---|---|
| | 2020 | 2021 | 2020 | 2021 |
| January | | -41.27 | | -71.70 |
| February | | -40.41 | | -62.05 |
| March | | -43.50 | | -64.71 |
| April | -42.20 | -37.56 | -62.11 | -58.86 |
| May | -40.56 | -43.81 | -63.00 | -64.01 |
| June | -42.28 | -39.91 | -61.98 | -60.39 |
| July | -41.97 | -43.00 | -64.92 | -62.07 |
| August | -40.07 | -40.63 | -63.15 | -61.42 |
| September | -42.53 | -41.57 | -63.57 | -61.25 |
| October | -43.55 | -45.15 | -64.80 | -61.81 |
| November | -53.86 | -38.26 | -67.95 | -64.34 |
| December | -54.89 | -41.20 | -70.32 | -67.84 |
| Average | -44.66 | -41.36 | -64.64 | -63.37 |

Source: Processed by Author

Additional regions with different intervention timings are summarized in the following table.

**Table 3.** Magnitude of NTL on Region Affected by First and Second Interventions with Different Intervention Effects (percent)

| Month | Gianyar | | Denpasar | | Karangasem | | Klungkung | |
|---|---|---|---|---|---|---|---|---|
| | 2020 | 2021 | 2020 | 2021 | 2020 | 2021 | 2020 | 2021 |
| January | | 210.48 | | -86.59 | | -0.69 | | 5.55 |
| February | | 1.41 | | -27.15 | | -68.96 | | -55.52 |
| March | | -15.55 | | -20.60 | | 14.12 | | 0.79 |
| April | -38,00 | -9.82 | -33.82 | -6.62 | -15.02 | 17.10 | -10,01 | -6.86 |
| May | -37.85 | -1.74 | -33.66 | 6.90 | -9.30 | 18.62 | -27.60 | 11.68 |
| June | -40.17 | 9.91 | -35.43 | 9.64 | -13.64 | 13.06 | -32.59 | 13.24 |
| July | -39.10 | 15.54 | -32.35 | 14.67 | -15.32 | 3.94 | -31.33 | 17.84 |

| Month | Gianyar | | Denpasar | | Karangasem | | Klungkung | |
|---|---|---|---|---|---|---|---|---|
| | 2020 | 2021 | 2020 | 2021 | 2020 | 2021 | 2020 | 2021 |
| August | -39.08 | 14.71 | -31.01 | 7.26 | -20.74 | -0.53 | -27.87 | 18.25 |
| September | -39.94 | 10.36 | -32.41 | 7.00 | -16.81 | 2.32 | -33.57 | 8.41 |
| October | -40.88 | 9.97 | -33.86 | 10.71 | -13.06 | -1.50 | -28.46 | 3.78 |
| November | -41.99 | 3.11 | -43.24 | -7.08 | -8.71 | 2.19 | -22.67 | 7.48 |
| December | -46.10 | -20.08 | -39.05 | -24.36 | -7.90 | 4.95 | -27.83 | 6.30 |
| Average | -40.35 | 19.03 | -34.98 | -9.68 | -13.39 | 0.38 | -26.88 | 2.58 |

Source: Processed by Author

Subsequent regions included in the analysis are presented in the next table.

**Table 4.** Magnitude of NTL on Region Affected Only by second Intervention (percent)

| Month | Tabanan | Jembrana | Buleleng | Bangli |
|---|---|---|---|---|
| January | -43.36 | -83.33 | -2.94 | 67.17 |
| February | -19.64 | -85.96 | -87.16 | 7.22 |
| March | -9.8 | -3.28 | -9.68 | -9.12 |
| April | -5.37 | -11.03 | -12.27 | 4.4 |
| May | -2.45 | 3.65 | -5.68 | 4.13 |
| June | -0.93 | 18.92 | 4.81 | 9.69 |
| July | -0.07 | 5.11 | 0.72 | 14.33 |
| August | 0.27 | -1.33 | -1.57 | 18.2 |
| September | 0.22 | -1.63 | 1.77 | 16.74 |
| October | 0.33 | -1.85 | 4.98 | 11.43 |
| November | -0.81 | 4.81 | 2.3 | 12 |
| December | -1.07 | 6.21 | -15.45 | 20.48 |
| Average | -6.89 | -12.48 | -10.01 | 14.72 |

Source: Processed by Author

In general, Bali experienced a decrease in NTL by -44.66% for the year 2020. This decrease in light intensity was instantaneous. This can be evidenced by the immediate drop that occurred during the implementation of PSBB in April. Additionally, based on the impact magnitude calculations in Table 2, it can be said that the change is permanent. This permanence is evident from the difference between the actual data and the prediction, which ranges around an average of -44.66%. Furthermore, the implementation of community activity restrictions also continues to show its impact on NTL. This can be observed from the difference between the prediction and actual data for 2021, which still hovers around 41.36%. The permanent and instantaneous impact of restrictions on NTL for 2020 also occurred in the regencies of Badung. This region experienced changes within their average ranges. The average magnitude of NTL changes in Badung was the highest compared to other regions.

Unlike Badung which still has a permanent impact from the first intervention, the group of regions consisting Denpasar, Gianyar, Karangasem and Klungkung, showed different response in 2021 when PPKM was implemented. Although experiencing same permanent effect in 2020, it can be seen from Table 3 that the effect on this

group of regions tend to decay two to three months after second intervention. The annual average magnitude NTL of this group also decreasing, meaning the restriction effect is slowly not taking effect after 2021. The highest pulse effect was on January 2021 in Gianyar. It may be caused with the presence of the outlier in the NTL data. The group of Tabanan, Jembrana, Buleleng, Bangli, and Karangasem showing another different intervention effect. It can be observed from Table 3, in this group, the intervention only takes effect on second restriction. The restriction impact negatively to NTL value on Tabanan, Jembrana, and Buleleng, while Bangli mostly experienced increase in NTL value.

If we observe the GHSL map for the built-up area in Figure 1, Badung, Gianyar, and Denpasar, located in the southern part of Bali, are areas with the highest built-up areas in Bali. This can be seen from the grouping of NTL images resulting from masking with GHSL that clustered in the south. At the same time, a significant decrease in light intensity was observed in these areas. With the significant decrease in light intensity, it can be said that activities in public places were truly limited to the residential areas. This is also reinforced by the statement from Mardika, Putra, and Wisnumurti (2020) that community activity restrictions were also monitored by *pecalang* to ensure the reduction of virus transmission. Therefore, it can be said that the decrease in NTL represents a decrease in human activity.

Furthermore, the decrease in NTL in Bali province is also in line with the decline in domestic and international tourists visiting Bali. Data sourced from BPS dynamic tables accessed in 2022 shows a drastic drop from previously 6,275,210 international tourist in 2019 to 1,069,473 person in 2020, while in 2021, only 51 persons. As widely known, Bali is an area with potential in tourism, including natural and cultural attractions. However, the pandemic indirectly halted tourism activities. Additionally, the closure of airports and flight restrictions as an effort to curb virus spread also further impacted tourism activities. This can be mainly observed from the activities in the buffer zones of Denpasar city, namely Badung, Gianyar, and Tabanan, which serve as buffer areas and were visibly affected by this decline. Referring to the research of Karimah and Yudhistira (2020), changes in light intensity reflect the socio-economic activities in the buffer zones around the ports; the results of this research align with that, but with larger buffer areas.

## 4. Conclusion

This study demonstrates that NTL remote sensing, as an alternative data can be used to assess socioeconomic disruption events like COVID-19. The temporal dynamics elements in NTL can also be used to observe near real-time monitoring of policy impacts, enabling data-driven decisions, and used to enrich the official statistics. The NTL has similar properties to official statistics, namely, GDP based on the quarterly movement. In addition, it can show human activity.

Although having a timely data than official statistics, the existence of outliers in NTL data due to poor quality images will result in problems in the modelling process, therefore, improvements need to be made to the available data. In this study, improvements were made to the processed data without masking the image. Therefore, further research requires a comparison between the improved data with the time series method and the masking method.

For policymakers, the existence of proxy data sources can be used as a reflection of the policies they make. Especially when official statistics are not yet available. In

addition, proxy indicators can also be used to carry out early detection of emergency policies so that policies do not have a negative impact and are beneficial to the community. For producers of official statistics, proxy data can be used as a complement to the information available from the data, so that it can be used as an insight into the phenomena that occur in the field.

## References

[1] Almutaqi, A. (2020). Kekacauan Respons terhadap COVID-19 di Indonesia. pp. 1-7. Retrieved from https://www.habibiecenter.or.id/img/publication/66f28c42de71fefe1c6fcdee37a5c1a6.pdf

[2] As-syakur, A. R., Ariastina, W. G., Kumara, N. I., Antara, I. M., Osawa, T., & Cahyani, D. A. (2021). Impact of Covid-19 Pandemic on Electricity Consumption and Nighttime Lights Based on NPP-VIIRS DNB Image Products. *2021 International Conference on Smart-Green Technology in Electrical and Information Systems (ICSGTEIS)* (pp. 161-164). IEEE.

[3] Awirya, A., Novita, D., Irawadi, C., & Wilandari, R. (2022). Workers Adaptation during Pandemic, Evidence from Bali Province as Main Tourist Destination in Indonesia. *e-Journal Ekonomi Bisnis dan Akuntansi*, 14-22.

[4] Box, G., Jenkins, G., Reinsel, G., & Ljung, G. (2015). *Time series analysis: forecasting and control.* John Wiley and Sons.

[5] BPS. (2022). *Banyaknya Wisatawan Mancanegara ke Bali Menurut Kawasan.* Retrieved from https://bali.bps.go.id/indicator/16/129/1/banyaknya-wisatawan-mancanegara-ke-bali-menurut-kawasan.html

[6] Cohen, J. (1988). *Statistical power analysis for the behavioral sciences.* Lawrence Erlbaum Associates.

[7] Devkota, B., Miyazaki, H., Witayangkurn, A., & Kim, S. (2019). Using Volunteered Geographic Information and Nighttime Light Remote Sensing Data to Identify Tourism Areas of Interest. *Sustainability, 11*(17), 4718.

[8] Elvidge, C., Baugh, K., Zhizhin, M., Hsu, F., & Tilottama, G. (2017). VIIRS Night-Time Lights. *International Journal of Remote Sensing*, 5860-5879.

[9] Field, A. (2018). *Discovering statistics using IBM SPSS statistics.* Sage publications.

[10] Gorelick, N., Hancher, M., Dixon, M., Ilyuschenko, S., Thau, D., & Moore, R. (2017). Google Earth Engine: Planetary-scale geospatial analysis for everyone. *Remote Sensing of Environment*, 18-27. Retrieved from https://www.sciencedirect.com/science/article/pii/S0034425717302900

[11] Haavelmo, T., & Hansen, S. (1991). On the Strategy of Trying to Reduce Economic Inequality by Expanding the Scale of Human Activity. In *Environmentally Sustainable Economic Development: Building on Brundtland* (pp. 41-49). Retrieved from https://documents1.worldbank.org/curated/en/332821467989482335/pdf/multi-page.pdf

[12] Han, G., Zhou, T., Sun, Y., & Zhu, S. (2022). The relationship between night-time light and socioeconomic factors in China and India. *PLOS ONE (17)1: e0262503*.

[13] Hyndman, R. J., & Khandakar, Y. (2008). Automatic Time Series Forecasting: The forecast Package for R. *Journal of Statistical Software, 27(3)*, 1–22.

[14] Karimah, I. D., & Yudhistira, M. H. (2020). Does small-scale port investment affect local economic activity? Evidence from small-port development in Indonesia. *Economic of Transportation 23*.

[15] Kopp, T. J., Thomas, W., Heidinger, A. K., Botambekov, D., Frey, R. A., Hutchinson, K. D., . . . Reed, B. (2014). The VIIRS Cloud Mask: Progress in the first year of S-NPP toward a common cloud detection scheme. *JGR Atmosphere*, 2441-2456. doi:https://doi.org/10.1002/2013JD020458

[16] Levin, N., Kyba, C., Zhang, Q., de Miguel, A., Roman, M., Xi, L., & Elvidge, C. (2020). Remote

sensing of night lights: a review and an outlook for the future. *Remote Sensing of Environment*, 111443. Retrieved from https://www.sciencedirect.com/science/article/abs/pii/S0034425719304626?via%3Dihub

[17] Li, X., Li, D., Xu, H., & Wu, C. (2017). Intercalibration between DMSP/OLS and VIIRS night-time light images to evaluate city light dynamics of Syria's major human settlement during Syrian Civil War. *International Journal of Remote Sensing*, 5934-5951.

[18] Makridakis, S. G., Wheelwright, S. C., & Hyndman, R. J. (1997). *Forecasting Methods and Applications Third Edition.* Hoboken: Wiley.

[19] Makridakis, S., Wheelwright, S., & Hyndman, R. (1997). *Forecasting Methods and Applications* (Third Edition ed.). Hoboken: Wiley.

[20] Mardika, I. M., Putra, I. B., & Wisnumurti, A. A. (2020). Pemberdayaan Pecalang Desa Adat Sumerta dalam Penanggulangan Covid-19. *Postgraduated Community Service Journal, 1 (2)*, 37-42.

[21] Mellander, C., Lobo, J., Stolarick, K., & Matheson, Z. (2015). Night-Time Light Data: A Good Proxy Measure for Economic Activity? *PLOS ONE 10(10): e0139779*.

[22] Montgomery, D. C., Jennings, C. L., & Kulahci, M. (2015). *Introduction to Time Series Analysis and Forecasting Second Edition.* New Jersey: Wiley.

[23] Montgomery, D., Jennings, C., & Kulahci, M. (2015). *Introduction to Time Series Analysis and Forecasting* (Second Edition ed.). New Jersey: Wiley.

[24] Pankratz, A. (1983). *Forecasting with Univariate Box-Jenkins Models: Concepts and Cases.* Greencastle: John Wiley and Sons.

[25] Pesaresi, M., Corbane, C., Julea, A., Florczyk, A. J., Syrris, V., & Soille, P. (2016). Assessment of the Added-Value of Sentinel-2 for Detecting Built-up Areas. *Remote Sensing*, 299. Retrieved from https://www.mdpi.com/2072-4292/8/4/299

[26] Pesaresi, M., Ehrlich, D., Ferry, S., Florczyk, A. J., Freire, S., Halkia, M., . . . Syrris, V. (2016). *Operating procedure for the production of the Global Human Settlement Layer from Landsat data of the epochs 1975, 1990, 2000, and 2014.* Italy: European Commission.

[27] Pesaresi, M., Ehrlich, D., Ferry, S., Florczyk, A., Freire, S., Halkia, M., & Syrris, V. (2016). *Operating procedure for the production of the Global Human Settlement Layer from Landsat data of the epochs 1975, 1990, 2000, and 2014.* Italy: European Commission.

[28] Shmueli, G., & Lichtendahl Jr., K. (2016). *Practical Time Series Forecasting with R: A Hands-on Guide.* Axelrod Schnall.

[29] Shmueli, G., & Lichtendahl Jr., K. C. (2016). *Practical Time Series Forecasting with R: A Hands-on Guide.* Axelrod Schnall.

[30] WHO. (2020). *Novel Coronavirus (2019-ncov) Situation Report - 1.* Retrieved from https://apps.who.int/iris/bitstream/handle/10665/330760/nCoVsitrep21Jan2020-eng.pdf?sequence=3'isAllowed=y

[31] World Bank. (n.d.). *1. Time Series Charts*. Retrieved from Open Night Light: https://worldbank.github.io/OpenNightLights/tutorials/mod4_1_time_series_charts.html

[32] Ye, J., Xiao, C., Esteves, R., & Rong, C. (2015). Time series similarity evaluation based on Spearman's correlation coefficients and distance measures. *Cloud Computing and Big Data: Second International Conference, CloudCom-Asia 2015, Huangshan, China, June 17-19, 2015, Revised Selected Papers 2* (pp. 319-331). Springer International Publishing.

[33] Zhao, N., Liu, Y., Hsu, F., Samson, E., Letu, H., Liang, D., & Cao, G. (2020). Time series analysis of VIIRS-DNB nighttime lights imagery for change detection in urban areas: A case study of devastation in Puerto Rico from hurricanes Irma and Maria. *ScienceDirect*.

**Appendix 1.** ARIMA Intervention Model for each Region in Bali

| |
|---|
| Bali<br>$y_t = \frac{(1+\theta_1 B)(1+\Theta_1 B^{12})}{(1-\Phi_1 B^{12})(1-B)}\varepsilon_t + \omega_0^{(76)} S_t^{(76)}$ |
| Badung<br>$y_t = \frac{(1+\theta_1 B)(1+\Theta_1 B^{12})}{(1-\Phi_1 B^{12})(1-B)}\varepsilon_t + \omega_0^{(76)} S_t^{(76)}$ |
| Bangli<br>$y_t = \frac{(1+\theta_1 B)(1+\Theta_1 B^{12})}{(1-\Phi_1 B^{12})(1-B)}\varepsilon_t + \left(\omega_0^{(85)} + \omega_1^{(85)} B\right) P_t^{(85)}$ |
| Buleleng<br>$y_t = \frac{(1+\theta_1 B+\theta_2 B^2+\theta_3 B^3)}{(1-\Phi_1 B^{12})(1-B)}\varepsilon_t + \omega_0^{(85)} B * P_t^{(85)}$ |
| Gianyar<br>$y_t = \frac{(1+\theta_1 B)(1+\Theta_1 B^{12})}{(1-\Phi_1 B^{12})(1-B)}\varepsilon_t + \omega_0^{(76)} S_t^{(76)} + \omega_0^{(85)} P_t^{(85)}$ |
| Jembrana<br>$y_t = \frac{(1+\theta_1 B+\theta_2 B^2)}{(1-\Phi_1 B^{12}-\Phi_2 B^{24})(1-B^{12})}\varepsilon_t + \left(\omega_0^{(85)} - \omega_1^{(85)} B\right) P_t^{(85)}$ |
| Karangasem<br>$y_t = \frac{(1+\theta_1 B+\theta_2 B^2+\theta_3 B^3)}{(1-\Phi_1 B^{12}-\Phi_2 B^{24})(1-B)}\varepsilon_t + \frac{\omega_0^{(76)}}{(1-\delta_1^{(76)} B)} P_t^{(76)} + \omega_0^{(85)} B * P_t^{(85)}$ |
| Klungkung<br>$y_t = \frac{(1+\theta_1 B)(1+\Theta_1 B^{12})}{(1-\Phi_1 B^{12})(1-B)}\varepsilon_t + \omega_0^{(76)} B * S_t^{(76)} + \omega_0^{(85)} B * P_t^{(85)}$ |
| Tabanan<br>$y_t = \frac{(1+\theta_1 B)}{(1-\Phi_1 B^{12})(1-B)(1-B^{12})}\varepsilon_t + \frac{\omega_0^{(85)}}{(1-\delta_1^{(85)} B)} P_t^{(85)}$ |
| Denpasar<br>$y_t = \frac{(1+\theta_1 B)(1+\Theta_1 B^{12})}{(1-\Phi_1 B^{12})(1-B)}\varepsilon_t + \omega_0^{(76)} S_t^{(76)} + \frac{\omega_0^{(85)}}{(1-\delta_1^{(85)} B)} P_t^{(85)}$ |